PERGAMON

International Journal of Heat and Mass Transfer 44 (2001) 1223–1233

International Journal of HEAT and MASS TRANSFER

www.elsevier.com/locate/ijhmt

# The heat/mass transfer analogy factor, *Nu*/*Sh*, for boundary layers on turbine blade profiles

E.R.G. Eckert, H. Sakamoto, T.W. Simon *

*Department of Mechanical Engineering, Heat Transfer Laboratory, University of Minnesota, 125 Mechanical Eng. Bldg., 111 Church Street S.E., Minneapolis, MN 55455, USA*

Received 4 February 2000; received in revised form 24 April 2000

**Abstract**

Heat transfer to gas turbine blades occurs at high Reynolds numbers, therefore in thin boundary layers. This makes the measurement of local heat transfer coefficients or Nusselt numbers difficult and suggests to measure mass transfer coefficients or Sherwood numbers instead. These are then transformed to Nusselt numbers by the heat/mass transfer analogy.

The present paper extends this analogy to processes in which the Schmidt number for mass transfer is not equal to the Prandtl number for heat transfer, by use of general fluid mechanics and transfer relations for boundary layers and explores what equations for the analogy can be derived in this way. The results are compared with computational and experimental information. 

## 1. Introduction

The heat/mass transfer analogy was developed by Schmidt [1] and Nusselt [2] (see also [3]) based on the conservation equations for momentum, heat and mass transfer of a constant property fluid for the purpose to transfer information from a heat transfer process to a physically and geometrically similar mass transfer process, and vice versa. For situations considered in the present paper, similarity is required for the following boundary conditions:

heat transfer: $Re$, $Pr$, $T_w$ or $q_w = \text{const}$, model shape;
mass transfer: $Re$, $Sc$, $c_w$ or $m_w = \text{const}$, model shape.

It is useful to distinguish in the description of a model (blade profile) between its size and its shape. The size is characterized by a selected prescribed length (for instance, the chord length, $C$, of the blade) and appears in the Reynolds number, $Re$, of the list of parameters given above. The shape is described by all necessary dimensionless lengths (for instance, $x/C$). The Nusselt number, $Nu$, as a dimensionless expression of the heat transfer coefficient and the Sherwood number, $Sh$, for the mass transfer coefficient, are then functions of those parameters.

They are also the dimensionless temperature or mass concentration gradients at the model surface.

$$Nu = \frac{\partial(T/\Delta T)_w}{\partial(n/C)_w}, Sh = \frac{\partial(c/\Delta c)_w}{\partial(n/C)_w}. \quad (1)$$

The two processes are, according to Schmidt and Nusselt, analogous for the two fluids when $Pr = Sc$ and, as a consequence,

$$Nu = Sh \text{ when } Pr = Sc. \quad (2)$$

This equation expresses the heat/mass transfer analogy.

A difficulty arises when the Prandtl number characterizing the heat transfer fluid is different from the Schmidt number characterizing the mass transfer fluid. This means that the condition in Eq. (2) is not fulfilled and the equation has to be changed to

$$Nu = F \cdot Sh \text{ when } Pr \neq Sc. \quad (3)$$

Similarity theory tells us only that the analogy factor, $F$, will be a function of the boundary conditions mentioned

* Corresponding author. Tel.: +1-612-625-5831; fax: +1-612-624-5230.
*E-mail address:* tsimon@me.umn.edu (T.W. Simon).

0017-9310/01/$ - see front matter 
PII: S0017-9310(00)00175-7

**Nomenclature**

| | |
|---|---|
| $C$ | chord length |
| $c$ | concentration |
| $c_p$ | specific heat |
| $D$ | mass diffusion coefficient |
| $F$ | local analogy factor, $F = Nu/Sh$ |
| $\bar{F}$ | spatially averaged analogy factor |
| $h$ | heat transfer coefficient, $h = q/\Delta T$ |
| $h_M$ | mass transfer coefficient |
| $k$ | thermal conductivity |
| $Nu$ | Nusselt number, $Nu = h \cdot C/k$ |
| $m$ | mass flux |
| $n$ | normal to surface |
| $Pr$ | Prandtl number, $Pr = \nu/\alpha$ |
| $P$ | pitch |
| $p$ | pressure |
| $q$ | heat flux |
| $Re_c$ | Reynolds number, $Re_c = U_e \cdot C/\nu$ |
| $Re_x$ | Reynolds number, $Re_x = U_s \cdot x/\nu$ |
| $Sc$ | Schmidt number, $Sc = \nu/D$ |
| $Sh$ | Sherwood number, $Sh = h_M \cdot C/D$ |
| $St$ | Stanton number, $St = h/\rho c_p U_s$ |
| $St_M$ | mass transfer Stanton number, $St_M = h_M/\rho c_p U_s$ |
| $T_w$ | blade surface temperature |
| $TI$ | turbulent intensity |
| $\Delta T$ | characteristic temperature difference |
| $U$ | velocity |
| $U_s$ | local velocity outside the boundary layer |
| $U_e$ | exit velocity |
| $u, v$ | velocity components $\bar{u}, \bar{v}$ |
| $\bar{u}, \bar{v}$ | time-averaged velocity components |
| $x, y, z$ | coordinates |

*Greek symbols*

| | |
|---|---|
| $\alpha$ | thermal diffusivity |
| $\alpha$ | upstream angle |
| $\delta$ | boundary layer thickness |
| $\delta_1$ | displacement thickness |
| $\varepsilon_M$ | turbulent diffusivity of momentum |
| $\mu$ | dynamic viscosity |
| $\nu$ | kinematic viscosity |
| $\rho$ | density |

*Subscripts*

| | |
|---|---|
| e | exit condition |
| in | inlet condition |
| M | mass transfer |
| ref | reference value |
| tr | transition |
| w | condition at blade surface |

above. Its usefulness depends on whether simple relations can be found for it.

There are three relations that are useful for an extended analogy, which are valid even when $Pr$ is different from $Sc$. They can be deduced from the Navier–Stokes, the heat transfer and the mass transfer equations and will be listed here but discussed in detail in the following sections of the paper.

(a) The Navier–Stokes equations with their boundary conditions can be solved for a constant property fluid without information on heat and mass transfer processes. The flow field in dimensionless form is independent of $Pr$ or $Sc$ of the fluid and depends only on the Reynolds number and the model shape. The velocity field influences the temperature or concentration field without itself being influenced.

(b) For a specified flow process, the functional relation between the temperature field and the concentration field in the differential equations describing a heat or mass transfer process is such that the equation for a heat transfer process can be converted into an equation for a mass transfer process by replacing the Prandtl number in the equation by the Schmidt number and the Nusselt number by the Sherwood number [4, p. 731]. This can be indicated by the operator

$$\frac{Sh}{\cancel{Nu}} \quad \frac{Sc}{\cancel{Pr}} = f(Re, \cancel{Pr}, \ldots) \tag{4}$$

The conversion works also from mass transfer to heat transfer. As an example, laminar heat transfer for steady, two-dimensional, boundary-layer flow over a flat plate with constant wall temperature can well be approximated by the equation

$$Nu_x = 0.332\sqrt{Re_x}\sqrt[3]{Pr} \quad \text{for } Pr > 0.6 \tag{5}$$

(see [4, p. 313]). Eq. (4) results in

$$Sh_x = 0.332\sqrt{Re_x}\sqrt[3]{Sc} \quad \text{for } Sc > 0.6 \tag{6}$$

and the analogy factor, $F$, for a prescribed Reynolds number is

$$F = \frac{Nu}{Sh} = \sqrt[3]{\frac{Pr}{Sc}}. \tag{7}$$

(c) Gas turbine blades operate at high Reynolds numbers, $Re_c$. Their boundary layers transport, therefore, information with high approximation in downstream direction only and Nusselt numbers are functions of $Re_x$ and $Pr$ when $Pr$ is of order one. The chord length, $C$, can be introduced as a dummy variable.

$$Nu_x = f(Re_x \cdot Pr) = f\left(\frac{U_s x}{\nu}, Pr\right) = f\left(\frac{U_s C}{\nu} \cdot \frac{x}{C}, Pr\right) = f\left(Re_c \cdot \frac{x}{C}, Pr\right). \tag{8}$$

The Sherwood numbers can be written according to (b).

$$Sh_x = f\left(Re_c \cdot \frac{x}{C}, Sc\right) \tag{9}$$

According to Eq. (7), the analogy factor for a laminar boundary layer flow on an isothermal surface at $U_s = \text{const}$ is independent of $x/C$, and it will be shown in Section 2 that this holds for other laminar boundary layers with varying velocities as well. According to the Eq. (A.8) in the Appendix A, it is expected to apply with good approximation to turbulent boundary layers also.

The following relation is, therefore, expected to hold generally for boundary layers at high Reynolds numbers, $Re_c$, when $Pr$ and $Sc$ are both of order one, a condition which is well established by gases (see [4, pp. 780, 782]).

$$\frac{Nu}{Sh} = f\left(\frac{Pr}{Sc}\right),$$

$$Nu = \left(\frac{\overline{Nu}}{\overline{Sh}}\right) Sh \quad \text{(independent of } x/C\text{)}. \tag{10}$$

The equation states that local Nusselt numbers are proportional to local Sherwood numbers with $\overline{Nu}/\overline{Sh}$ acting as proportionality factor. It should be straightforward to generalize relation (c) to three-dimensional problems.

In the following sections, the heat/mass transfer analogy will be studied in detail for laminar boundary layers by analysis and for turbulent boundary layers with recourse to experimental results as they exist on gas turbine profiles.

In the first section, analogy factors for two turbine blade profiles will be calculated for two-dimensional boundary layers as they exist on the central part of turbine blades where the flow and heat transfer are two-dimensional.

Experiments in which naphthalene vapor is transferred from solid naphthalene result in Sherwood numbers, and, by use of the heat/mass transfer analogy, they are converted into Nusselt numbers. The Prandtl number, $Pr$, for air at room temperature (300 K) is 0.707, and the Schmidt number of naphthalene vapor in mixture with air is 2.28. These values will be used for the numerical calculations.

## 2. Laminar boundary layers

The heat/mass transfer analogy is derived from the Navier–Stokes and the heat and mass transfer equations for a constant-property fluid. It will be used here for a steady, two-dimensional, laminar boundary layer, characteristic of the central part of the span of a turbine blade, using a coordinate system with $x$ measured in the flow direction from the stagnation line on the leading edge continuing along the airfoil suction surface. The $y$-coordinate is normal to it and away from the surface.

When incompressible and of moderate speed, the flow in the boundary layer is described by

$$\frac{\partial u}{\partial x} + \frac{\partial v}{\partial y} = 0, \tag{11}$$

$$\rho\left(u\frac{\partial u}{\partial x} + v\frac{\partial u}{\partial y}\right) = -\frac{\partial p}{\partial x} + \mu\frac{\partial^2 u}{\partial y^2}, \tag{12}$$

$$\frac{\partial p}{\partial y} = 0. \tag{13}$$

The boundary conditions are

$$\text{At } y = 0, \quad u = 0, \quad v = 0. \tag{14}$$

Diffusion of naphthalene creates flow away from the solid surface, but it is shown, by Goldstein and Cho [10–12], that the influence of this is very small and that $v = 0$ at $y = 0$ is a good approximation for the naphthalene experiments.

$$\text{As } y \to \infty, \quad u = U_s(x). \tag{15}$$

The velocity $U_s$ is a function of the pressure profile shape which, in turn, depends also on the pitch, $P$, of the airfoil cascade and the upstream flow conditions. The velocity, $U_s$, is usually calculated from the measured pressures around the blade surfaces.

The above equations with their boundary conditions can be solved for the velocity components, $u$ and $v$. The pressure, $p$, is obtained from the Bernoulli equation.

$$p + \rho\frac{U_s^2}{2} = \text{const}. \tag{16}$$

The parameter characterizing the shape of the turbine blade profiles in the boundary layer equations is the dimensionless velocity, $U_s/U_e$, as a function of the dimensionless distance, $x/C$, measured along the blade suction surface from the stagnation line. Such velocity profiles are available in the literature for two blade profiles. They will be used as characteristics for turbine blades. These shapes and flow characteristic are also reported in [5,6] for the profile denoted as S1 (1970s technology) and in [7] for the profile S2 (modern technology). Fig. 1 shows, for both blades, the dimensionless velocity, $U_s/U_e$, over the dimensionless distance, $x/C$, measured along the blade suction surface from the stagnation line. It can be observed that S1 has a very steep velocity increase close to the stagnation line and an almost constant velocity afterwards whereas the velocity increase of S2 extends over a considerable part of the blade chord length, $C$.

Eqs. (11)–(16) together with the velocity profiles are sufficient for the solution of the velocity field $(u, v)$ when the fluid properties, $\rho$ and $\mu$, are constant.

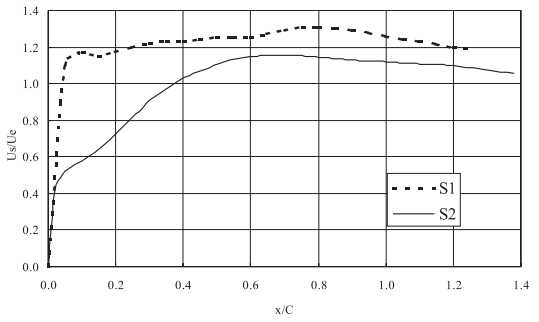


Fig. 1. Suction-surface velocity profile of S1 and S2 blades (S1 corresponds to a 1970s technology, and S2 corresponds to a modern technology).

Heat transfer in a laminar boundary layer is described by the equation

$$u\frac{\partial T}{\partial x}+v\frac{\partial T}{\partial y}=\alpha\frac{\partial^2 T}{\partial y^2}, \tag{17}$$

and mass transfer by

$$u\frac{\partial c}{\partial x}+v\frac{\partial c}{\partial y}=D\frac{\partial^2 c}{\partial y^2} \tag{18}$$

with the boundary conditions

$$T_w \text{ or } q_w = \text{ const}, \tag{19}$$

$$c_w \text{ or } m_w = \text{const}. \tag{20}$$

Actually, the heat transfer equation resulting in the Nusselt number, *Nu*, is sufficient because the Sherwood number can be obtained by Eq. (4).

The boundary condition $T_w = \text{const}$ is best suited for turbine blade analyses because the variation of the blade surface temperature, $T_w$, is generally small compared to the driving difference of the gas temperature in the mainstream and the mean temperature of the blade wall surface. $T_w = \text{const}$ is also equivalent to the boundary condition $c_w = \text{const}$ prevailing in the naphthalene experiment. On the other hand, the boundary condition $q_w = \text{const}$ is produced in a liquid crystal experiment which is frequently used to determine gas turbine heat transfer. It is, therefore, included in the following analysis.

The system of boundary layer equations with their geometric and boundary conditions was solved, using the TEXSTAN code [8], a parabolic boundary layer equation solver. The velocity profile for two-dimensional stagnation flow ($m = 1.0$ in Fig. 8 in Appendix A) served as boundary condition at $x/C = 0.00$ to start the velocity profile, $u$, for the S1 and S2 blade profiles. Calculation was continued in the $x$-direction until a velocity profile with $\mathrm{d}u/\mathrm{d}y = 0$ at $y = 0$ resulted, which indicated the start of flow separation. Calculations for a plane wall started with the Blasius profile at the leading edge.

Table 1 identifies the cases for which Nusselt numbers were calculated. Those numbered from 1 to 3 are for the blade profile S1. Computations were also made for a plane surface with $U_s = \text{const}$. They have the numbers 4–6. The boundary conditions for each case are arranged in a vertical column (*Pr* or *Sc*, $T_w$ or $q_w = \text{const}$). The same table can also serve for the blade profile S2 when S1 is replaced by S2 as the blade profile.

Analogy factors, *Nu*/*Sh*, can now be obtained for any combination of case numbers and are denoted by the ratio of two numbers with the first one assigned to the case with $Pr = 0.707$.

The temperature dependence of the Prandtl and Schmidt numbers is very weak. Both change, near room temperature, only by 0.5% for a 10°C temperature difference. Eq. (7) can, therefore, be simplified for a laminar boundary layer over a flat plate with constant velocity, $U_s$, to

$$F=\frac{Nu}{Sh}=0.677 \tag{21}$$

to convert experiments with naphthalene ($Sc = 2.28$) to air near room temperature. The conversion of *Nu* of air from room temperature to combustion gases at temperatures occurring in gas turbines is a special consideration. It has been discussed by Eckert [9].

Analytical solutions exist for laminar boundary layers in "wedge-type flow". The analogy factor for those is reported in the Appendix A.

A few combinations of special interest will now be discussed.

(1) The thermal boundary condition, $c_w = \text{const}$, is prescribed for the naphthalene mass-transfer and $T_w = \text{const}$ for the air heat transfer. All other boundary conditions are assumed identical. Figs. 2–4 present *Nu*/*Sh* factors for the combination of a heat transfer process in air ($Pr = 0.707$) and a mass transfer process using naphthalene ($Sc = 2.28$) as a function of the

Table 1
Case numbers for which *Nu*/*Sh* curves are shown in Figs. 2–4

| Case | 1 | 2 | 3 | 4 | 5 | 6 |
|---|---|---|---|---|---|---|
| Profile | S1 | S1 | S1 | $U_s = \text{const}$ "plane wall" | | |
| *Sc* or *Pr* | 2.28 | 0.707 | 0.707 | 2.28 | 0.707 | 0.707 |
| BC | $T_w$ | $T_w$ | $q_w$ | $T_w$ | $T_w$ | $q_w$ |

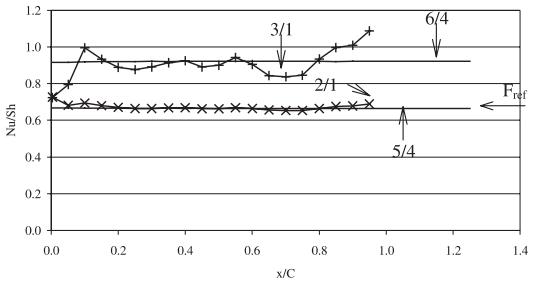


Fig. 2. Analogy factor $Nu/Sh$ for the S1 profile and the "plane wall" cases (Table 1) for laminar boundary layer, $Re_c = 171{,}000$ and $P/C = 0.77$ ($x/C = 1.25$ at the trailing edge), compared to the reference value, $F_{ref} = 0.677$, by Eq. (21).

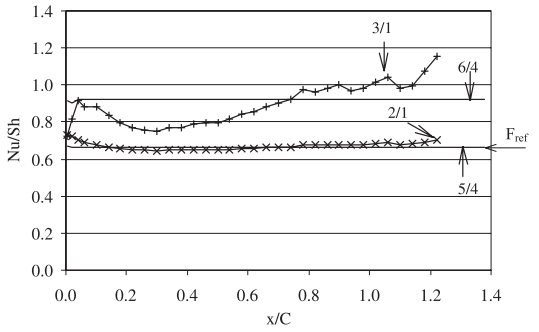


Fig. 3. Analogy factors, $Nu/Sh$, for the S2 profile and the "plane wall" cases (Table 1) for laminar boundary layer, $Re_c = 540{,}000$ and $P/C = 0.75$ ($x/C = 1.38$ at the trailing edge), compared to the reference value, $F_{ref} = 0.677$, by Eq. (21).

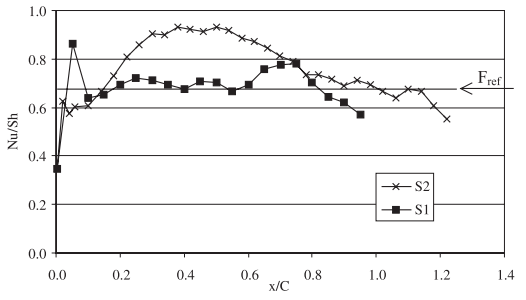


Fig. 4. Analogy factors, $Nu/Sh$, of the case 2/4 for both S1 and S2 profiles (Table 1) for laminar boundary layer, compared to the reference value, $F_{ref} = 0.677$ by Eq. (21).

dimensionless distance, $x/C$, along the profile suction surface. This combination is denoted as cases 5 and 4 in Table 1, or 5/4 in Fig. 2, when both processes are in flow over a plane surface (with $U_s = \text{const}$). In the Figs. 2–4, the analogy factor appears as a horizontal line at $Nu/Sh = 0.677$, the value already listed as Eq. (21). It will serve at a reference value, $F_{ref}$. In the same way, analogy factors for other boundary conditions identified in Table 1 can be evaluated, and their $Nu/Sh$ ratio can be entered in Figs. 2–4. The case number identifications for the profiles, S1 and S2, are cases 2 and 1, or 2/1, and the corresponding $Nu/Sh$ ratio has been entered in Figs. 2 and 3. It is astonishing and gratifying that, in both cases, the $Nu/Sh$ ratio agrees with excellent approximation with $Nu/Sh = 0.677$. The accuracy of the results of naphthalene experiments is listed in the literature as 5%. This accuracy is also obtainable for the Nusselt number and the heat transfer coefficients in turbine blade profiles.

(2) Many heat transfer experiments were performed to determine Nusselt numbers using the liquid crystal method which produces the thermal boundary condition of a constant heat flux at the wall surface ($q_w = \text{const}$). The results have been paired with those obtained by the naphthalene method producing a constant wall concentration boundary condition for turbulent boundary layers with the justification that turbulent flow minimizes the effect of the thermal boundary condition, according to experience. The $Nu/Sh$ ratio can now be calculated for laminar boundary layers. The case number identifications for these boundary conditions are found in Table 1 to be cases 3/1 for both profiles S1 and S2 and the corresponding $Nu/Sh$ ratio is plotted for S1 and S2 in Figs. 2 and 3. One observes that the $Nu/Sh$ ratio varies with the location on the surface which is inconvenient. The corresponding analogy factor for a plane surface is also calculated and entered in Figs. 2 and 3 as a horizontal line for cases 6/4. The mean value of the $Nu/Sh$ ratio is obviously also different from $F_{ref}$.

(3) It will now be explored how a difference in the shape of the blade model influences the analogy factor. Specifically, the heat transfer experiments will be assumed to be performed on a plane wall (at $U_s = \text{const}$) with the intention of determining the Nusselt numbers at the blade profiles S1 and S2.

The resulting $F = Nu/Sh$ values are presented in Fig. 4 together with the reference value 0.677. The fact that the model shape was varied in the analogy process has again the undesirable effect that the analogy factor varies along the model surface although to a smaller degree than a variation in the thermal boundary condition.

In summarizing the paragraphs (1)–(3), it can be stated that all pertinent boundary conditions should be set identical for the heat and mass transfer processes to be compared in an analogy when they are laminar boundary layers of gas turbine profiles.

This provides the advantage that Eq. (7) (or the constant 0.677 for the ratio $Nu/Sh$) can be used with excellent approximation for the analogy factor, $Nu/Sh$, for blade profiles with constant wall surface temperature. It also results in the analogy factor which is independent of $x$.

The summarizing statements above are as special cases in agreement with the relations (a)–(c) presented in the introduction and point out the importance of specifying all boundary conditions.

Of importance to gas turbine applications is the effect of elevated turbulence level. A systematic study of the influence of upstream turbulence on heat transfer to gas turbine blade profiles is due to Wang [7]. He used the S2 profile for his study and measured Sherwood numbers using the naphthalene sublimation method at Reynolds numbers between $2.41\times10^5$ and $7.51\times10^5$. He calculated Nusselt number profiles for two-dimensional, laminar boundary layers on a uniform temperature S2 blade and found good agreement between measured Sherwood numbers and calculated Nusselt numbers up to transition to turbulent flow when the upstream turbulence intensity was low (0.2%). With increasing upstream turbulence, the pre-transitional Sherwood number increased in such a way that the $Sh(x/C)$ profile shape remained essentially unchanged. This suggested that the boundary layer maintained its laminar character, for no abrupt changes indicating transition were observed.

## 3. Turbulent boundary layers

The basic heat/mass transfer analogy, Eq. (2), is derived for turbulent flow from the unsteady, three-dimensional Navier–Stokes, energy and mass concentration equations for a constant-property fluid in the same way as was done for the laminar boundary layers.

The equations contain, in addition to the large scale velocities, $u$, $v$ and $w$, small scale, high frequency velocity fluctuations describing turbulence. Their solutions would describe the velocity field in all its details including the turbulent fluctuations as a function of time. This is not yet possible today, but the equations are used to derive the basic heat/mass transfer analogy, Eq. (2) and the operator (4).

In engineering, we are primarily interested in time-averaged, steady relations for flow, heat and mass transfer parameters. Osborne Reynolds [10–12] obtained equations from which these parameters can be derived by averaging the Navier–Stokes equations over a time period which make the turbulent fluctuations disappear.

The continuity and momentum equations for a turbulent, steady, two-dimensional boundary layer of a constant property fluid assume, in this way, the form:

$$\frac{\partial\bar{u}}{\partial x}+\frac{\partial\bar{v}}{\partial y}=0, \tag{22}$$

$$\rho\left(\bar{u}\frac{\partial\bar{u}}{\partial x}+\bar{v}\frac{\partial\bar{u}}{\partial y}\right)=-\frac{\partial\bar{p}}{\partial x}+\rho\frac{\partial}{\partial y}\left[(\varepsilon_{\mathrm{M}}+\nu)\frac{\partial\bar{u}}{\partial y}\right], \tag{23}$$

in which the velocity components, $\bar{u}$ and $\bar{v}$, describe the macroscopic (large scale) velocities which, for steady flow, are independent of time whereas the turbulent fluctuations appear as shear stress, $\rho\varepsilon_{\mathrm{M}}\partial\bar{u}/\partial y$, where $\varepsilon_{\mathrm{M}}$ is called turbulent diffusivity of momentum. Similar terms appear in the heat and mass transfer equations. Nusselt, Sherwood numbers and analogy factors, $Nu/Sh$, can be obtained in this way when empirically obtained diffusivities are introduced into the boundary layer Eqs. (22) and (23).

Much effort has been spent in developing methods and equations by which the effects of turbulence structure on these diffusivities can be described for certain types of flow (boundary layers, free shear layers, jets). It has to be expected that these types serve as parameters (similar to boundary conditions for laminar flow). Nusselt and Sherwood numbers can thus be obtained by solving the turbulent boundary layer equations with the macroscopic boundary conditions – the same as for laminar flow – and the turbulent parameters.

This procedure is not used in the present paper; instead, the analogy factor will be based on measured Nusselt and Sherwood numbers.

*Developed turbulence*. An equation for the analogy factor for the standard flow with a steady uniform velocity, $U_{\mathrm{s}}=\mathrm{const}$, over a plane surface generating a turbulent two-dimensional boundary layer, starting at $x/C=0$, will be developed. The thermal boundary condition $T_{\mathrm{w}}=\mathrm{const}$ is prescribed. Many experimental and analytical studies of heat transfer have resulted in correlation equations. One of them listed by Eckert and Drake [4] describes the Stanton number, $St$, as a function of $Re$ and $Pr$ numbers.

$$St=\frac{0.0296Re_x^{-1/6}}{1+1.48Re_x^{-1/10}Pr^{-1/6}(Pr-1)}. \tag{24}$$

The Stanton number is related to the Nusselt number, $Nu_x$, by the relation

$$St=\frac{Nu_x}{Re_xPr}. \tag{25}$$

An equation for an equivalent mass transfer problem is obtained from Eq. (4), according to the heat/mass transfer analogy by replacing $Pr$ by $Sc$. Combining this and Eq. (25) results in the analogy factor

$$\frac{Nu}{Sh}=\frac{Pr}{Sc}\cdot\frac{1+1.48Re_x^{-1/10}Sc^{-1/6}(Sc-1)}{1+1.48Re_x^{-1/10}Pr^{-1/6}(Pr-1)}. \tag{26}$$

The length, $x$, does not appear in the ratio, $Nu/Sh$.

According to Goldstein and Cho [13], this leads, for a system consisting of naphthalene and air, to the following relation

$$\frac{Nu}{Sh}=0.5\ \text{ at } Re_x=10^6 \tag{27}$$

with $Nu/Sh$ larger by about 10% at $Re_x = 10^5$ and smaller by about 10% at $Re_x = 10^7$.

Eq. (27) is obtained by setting $Pr = 0.707$ and $Sc = 2.28$. The Stanton number in Eq. (24) is independent of chord length, $C$, and the analogy factor is, therefore, independent of $x/C$, according to the relation (c) in the introduction. It, therefore, is restricted to these two fluids and to near room temperatures. It is frequently used for turbulent boundary layers on gas turbine profiles with the justification that turbulent mixing diminishes the effects of velocity gradients along the blade surfaces.

The critical Reynolds number for transition to turbulence is of order $10^5$ and no smaller values of $Re_x$ need to be considered in Eq. (26).

Häring and Weigand [14] developed, by analysis for the turbulent boundary layer on a plane wall, an equation which describes the analogy factor. For small Mach numbers, it reduces to

$$\frac{Nu}{Sh} = \left(\frac{Pr}{Sc}\right)^{0.6526} \tag{28}$$

with $Pr/Sc = 0.707/2.28$, this relation results in

$$\frac{Nu}{Sh} = 0.466. \tag{29}$$

Heat transfer coefficients obtained with the equations derived by Häring and Weigand [14] were, for instance, compared by Häring et al. [15] and Hoffs et al. [16] with experimental results obtained in turbine blade cascades. The data agreed moderately well.

A new boundary condition has to be introduced when transition to turbulence occurs at a value $x/C > 0$. A transitional Reynolds number, $Re_{tr}$, characterizes this and $x_{tr}/C$ establishes the location for the start of a turbulent boundary layer. The analogy factor is constant for the laminar boundary layer with a value 0.677 for $Pr = 0.707$ and $Sc = 2.28$ up to $Re_{tr}$ and with a value 0.5 downstream of transition. In reality, the transition point is replaced by a transition range in which $Nu/Sh$ changes from 0.677 to 0.5.

*Developing turbulence*. Eqs. (26)–(29) are based on the assumption that convective heat or mass transfer is dominating in fully developed turbulence. There are also regions on turbine blades where conduction or diffusion cannot be neglected. Detailed and accurate information on local Nusselt numbers is required. Those are, however, difficult to obtain, especially in three-dimensional boundary layers. Therefore, another method is proposed which is based on Eq. (10).

*Local Sherwood numbers are measured in an experiment in which naphthalene vapor is transferred by diffusion and convection into an air stream. Average Sherwood numbers are also measured by weighing or by integration of the local results. Average Nusselt numbers, much easier to measure than local ones, are measured on a blade model with high conductivity producing a constant wall temperature in a separate experiment and Eq.* (10) *is used to obtain the desired local Nusselt numbers.*

There is also experimental evidence of the validity of this equation for various types of flow.

Goldstein and Cho [13] presented, in their Figs. 13–15, Nusselt and Sherwood numbers along the surfaces of round, square, and rectangular cylinders in cross-flow. It can be observed that, in these figures, $Nu$ is nearly proportional to $Sh$, which means that the mean analogy factor, $\bar{F}$, averaged over the surface, is nearly equal to the local factor, $F$.

## 4. Three-dimensional boundary layers

The boundary layers discussed up to this point are two-dimensional. There are, in the literature, two papers with data that make it possible to test analogy factors for application to three-dimensional turbulent boundary layers, as they occur in the near-endwall region of gas turbine blades.

The heat transfer experiments (e.g., Chung and Simon [17] and Chung [18]) used the liquid crystal technique (a uniform heat flux boundary condition) and the mass transfer experiment (e.g., Chen [5] and Chen and Goldstein [6]) applied the naphthalene sublimation technique (equivalent to a uniform wall temperature boundary condition). The experiments produced fields of Stanton numbers and mass-transfer Stanton numbers on the S1 blade shape.

Table 2 summarizes relevant parameters of the experiments. It lists the approach velocity, $U_{in}$, turbulent intensity, $TI$, Reynolds number at the entrance to the cascade, $Re_{in}$, as well as Reynolds number at the exit, $Re_{ex}$, the pitch-to-chord-length ratio, $P/C$, and the ratio of wall boundary layer thickness to the chord length at the cascade entrance, $\delta_1/C$, among other parameters.

One important difference between the heat and mass transfer cases is in the boundary conditions; the heat

Table 2
Comparison of the experiments

| | Mass transfer [5,6] | Heat transfer [18,17] |
|---|---|---|
| $U_{in}$ (m/s) | 10.45 | 20 |
| $TI$ (%) | 1.31 | 0.6 |
| $Re_{in}$ | 104,000 | 293,000 |
| $Re_{ex}$ | 171,000 | 482,000 |
| Profile | S1 | S1 |
| BC[a] | $T_w = \text{const}$ | $q_w = \text{const}$ |
| $P/C$ | 0.77 | 0.77 |
| $\delta_1/C$ | 0.013 | 0.013 |

[a] BC: boundary condition.

transfer experiment is of a uniform heat flux and the mass transfer experiment is of a uniform film mass concentration at the surface (saturation at the uniform temperature of the surface). This difference in thermal boundary condition was shown in Section 2 to have an effect on the laminar region but is generally assumed to have only a minor effect on the turbulent flow region. This will also be assumed in our evaluation of their results.

*Mass transfer experiment*. The data from Chen and Goldstein [6] are recorded as mass transfer Stanton numbers. The study presents data with two different sizes of displacement thickness in the boundary layer of the approaching flow. For the present study, the case in which the displacement thickness, $\delta_1$, used was 1.3% of the chord length (2.13 mm). The uncertainty in mass transfer Stanton number of their naphthalene experiments is reported to be 5%. These data, converted to Sherwood number, are plotted in Fig. 5 for the suction surface of the S1 blade profile.

The abscissa $x/C$ of the figure extends from the stagnation line ($x/C = 0$) in downstream direction, measured along the blade surface. The ordinate $z/C$ extends from the corner between the endwall and the blade surface ($x/C = 0$) to a distance $z/C = 0.75$ from the endwall measured along the blade wall. Fig. 5, therefore, covers a part of the wall where the boundary layer is influenced by the passage vortex systems (the essentially triangular part limited by a line extending from $x/C = 0$, $z/C = 0$ to approximately $x/C = 1.35$, $z/C = 0.4$) and the rest of the wall where the boundary layer is essentially not affected by the endwall and can be considered as two-dimensional. This part of the boundary layer starts changing to turbulent flow approximately at a distance $x/C = 1$. A boundary layer of laminar character starts at the leading edge of the blade to the left and fills the central part changing to turbulence at the transition region characterized by the lines of constant $St_m$ number. The boundary of this region moves left with decreasing $z/C$ about halfway down the figure under the influence of the passage vortex.

The description above is believed to cover the main features of the boundary layer flow. There are certainly minor details which are omitted.

*Heat transfer experiment*. Chung [18] presents the photograph of a liquid crystal sheet that had been glued to the suction surface of a S1 blade model and exposed to the airflow through a cascade of the same blades. The photograph was digitized by the present authors using a scanner. As noted by Camci et al. [19], a wide range of hue has a linear relationship with temperature. Thus, a linear relation was used to determine surface temperature distribution. The scanned photograph was first recognized as an RGB image (consisting of Red, Green and Blue). This was then converted to an HSV image (Hue, Saturation and Value), using the commercially available MATLAB program. Since the temperatures at the colors of yellow and green were known from the calibration and since the wall heat flux was known, the entire region of the photograph could be converted into a field of Nusselt numbers. The original size of $334 \times 353$ pixels scanned at 100 pixels/inch was scaled down to $83 \times 88$, as noise was reduced. Fig. 6 presents the result. Temperatures resulting in contours of 0.004 or more were at the edge of the liquid crystal color transition. Their accuracies are therefore questionable.

The *Nu* values of the heat transfer experiment were divided by the *Sh* number values (converted from $St_m$ values) of the mass transfer experiment to get the *Nu*/*Sh* values plotted in Fig. 7. Prior to the division which resulted in *Nu*/*Sh* of Fig. 7, the *Nu* field was shifted slightly with respect to the *Sh* field, obtained from Fig. 5, so that the triangular regions created by the vortex matched. This affects only the data on that line of very steep gradient (a line from 0.27, 0.8–0.5, 1.33 in Fig. 7). It is

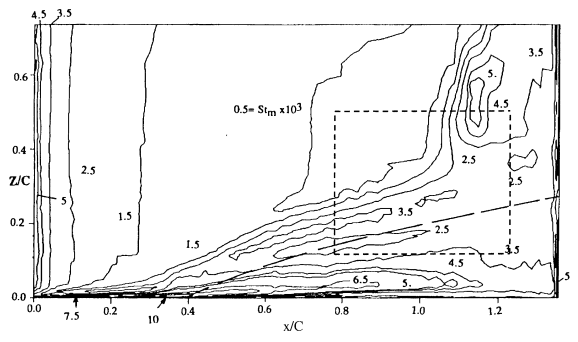


Fig. 5. Mass transfer Stanton number distribution from the mass transfer experiment on the S1 airfoil profile, the dashed line indicates the rectangular fields of Figs. 6 and 7 [5, 6].

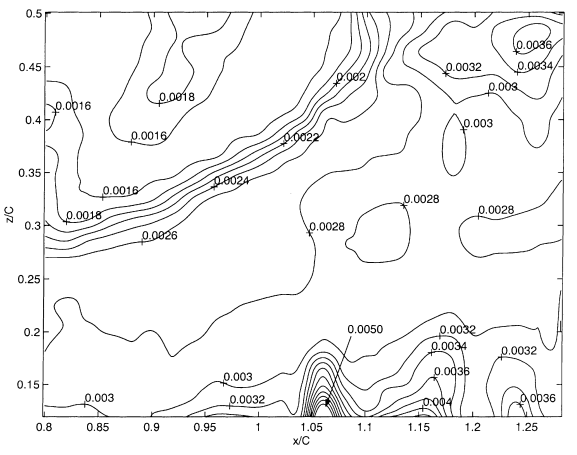


Fig. 6. Stanton number distribution calculated from the liquid crystal photograph taken on the S1 airfoil profile [18].

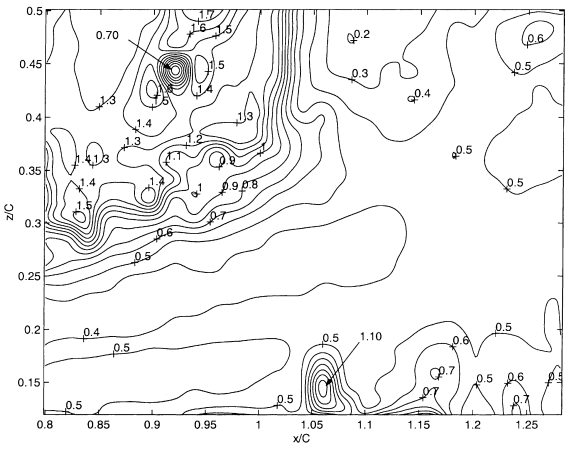


Fig. 7. $Nu/Sh$ near the corner of the endwall and trailing edge on the S1 airfoil profile.

not known why the triangular regions do not match precisely but it is not surprising that they shifted slightly from one test setup to the other. The near-endwall region data are expected to depend on the approach flow boundary layer thickness, free-stream turbulence intensity and, undoubtedly, other factors. The axes shown in the Figs. 6 and 7 correspond to those of the mass transfer experiment.

The very first point to notice in Fig. 7 is that the ratios vary over a range, from below 0.4 to about 1.0. The larger values are in a flow that appears to be transitional. The ratio 0.40–0.50 in the center field at right are where the turbulent boundary layers are expected.

The following difficulty is encountered in interpretation and evaluation of the data in Figs. 5–7. It is the intent of this study to obtain time-averaged information for macroscopically steady, turbulent flow. Clearly, some of the contour lines in these figures are not the ones we expect for steady state and for a configuration of straight blades normal to a plane endwall, contour lines, as they would, for instance, be produced by a solution of the time-averaged Navier–Stokes equations for turbulent flow. Stationary circular formations as shown in Fig. 7 along the lower rim of the field and its upper left corner or stationary waves as shown in the boundary layers with large gradients are suspect.

One can list several reasons which explain these differences.

The time interval during which the data were averaged in the two experiments may not be long enough to create steady data. In the naphthalene study, it is usually of order 1/2 h. In the liquid crystal study, it is much shorter, of the order of a second. That this influences the contour lines is supported by the fact that Fig. 5 resembles more the expected steady contour map than Fig. 7 which also displays the regions pointed out above. Other contour maps in [7] or in [20] resemble Fig. 5.

The two studies on which Fig. 7 is based have not been planned for the purpose to determine analogy factors. This influenced the accuracy with which we could coordinate these and made a slight adjustment necessary. This influences especially the regions with larger gradients of the $Nu/Sh$ field indicated by the crowding of the contour lines.

The difference in the thermal boundary conditions of the two studies is generally assumed to have a negligible influence in the turbulent region. However, the flow in the upper left parts of Figs. 5–7 is expected to be partially laminar, where there might be effects of different thermal boundary conditions.

It can be concluded from the observations above that the values of 0.4 and 0.5 in the central region of Fig. 7 are most reliable. This is an important finding, for the flow field there is more complex than those used in the formulation of Eqs. (27) and (29). We conclude that, for turbulent, three-dimensional boundary layers as they occur in the near-endwall region of gas turbine blades, the time-averaged analogy factors, $Nu/Sh$, have values in this range.

The wall in the upper-left of Fig. 7 is cooled by a laminar boundary layer. As it is laminar, there will be a thermal boundary effect. Also, it is experiencing an adverse pressure gradient. Thus, data in the figure have to be compared with the results of curve 3/1 in Fig. 2 for $x/C > 0.8$. The difference between the Fig. 7 values (in the 1.3–1.4 range) and the Fig. 2 values (as high as 1.1) may be explained by the fact that the calibration curves with which the Stanton numbers in Fig. 6 were obtained had to be extrapolated in this region.

Values between 0.5, typical of turbulent flows, and 1.1, computed for laminar flows, appear in the boundary layer transition zone of Fig. 7. This is consistent with a smooth transition from laminar to turbulent flow.

## 5. Conclusions

From this work, the following can be concluded:

The analogy factor, $Nu/Sh$, for two-dimensional laminar boundary layers is equal to $\sqrt[3]{Pr/Sc}$ and is constant along the front part of the blade wall making the Nusselt number proportional to the Sherwood number provided that all boundary conditions match for the heat and mass transfer processes and the flow velocities are such as to minimize aerodynamic heating.

This statement is based on relations derived from the Navier–Stokes and the heat and mass transfer equations for constant-property fluids and our solutions of the laminar boundary layer equation for wedge-shaped objects and turbine blade profiles. It is believed that they are valid for three-dimensional boundary layers also.

Analysis of laminar boundary layer equations for situations where either the thermal or the geometric

boundary conditions are violated resulted in analogy factors which do not agree with the relation $\sqrt[3]{Pr/Sc}$ and which vary locally. We believe that only those analogy factors should be used that were obtained either by analyses or by experiments in which all boundary conditions are fulfilled.

A reliable analogy factor was derived by numerous heat transfer experiments for a wide range of Prandtl numbers for turbulent flow at constant velocity $U_s$ over a plane surface with constant temperature. It is reported as Eq. (6). Its accuracy is estimated to be 10%. Goldstein and Cho [13] approximated it for $Pr = 0.707$ and $Sc = 2.28$ by $Nu/Sh = 0.5$ at $Re_c = 10^6$, larger by 10% at $10^5$ and smaller by 10% at $10^7$.

The fact that boundary layers transport information overwhelmingly in the downstream direction follows that the analogy factor is constant on regions of the model surface which have uniform turbulence structure. This is also in agreement with Fig. 7 of this paper. In the absence of better information, it is recommended to use the value 0.5 for the analogy factor when air is the heat transfer medium and naphthalene the mass transfer medium at $T_w = \text{const}$ and $c_w = \text{const}$, respectively, as wall boundary condition.

Information is lacking for analogy factors for separated flow regions and for film cooling. Measurements suggest a smooth transition of analogy factor from laminar to turbulent flow.

**Acknowledgements**

This study was performed with financial support by the Dean of the Institute of Technology of the University of Minnesota. Support was also provided by the Advanced Gas Turbine Systems Research Program, Clemson University under contract #CMU/541252-49598/DOE and by the US. Civilian Research and Development Foundation under award # UE 2-293. The authors are appreciative of the helpful suggestions offered by David Kercher of the General Electric Company.

## Appendix A

A special group of laminar boundary layers is called wedge flows in which the stream velocity, $U_s$, is described by the equation

$$U_s = cx^m. \tag{A.1}$$

The exponent, $m$, can be described by

$$m = \frac{x}{U_s}\frac{dU_s}{dx}. \tag{A.2}$$

The Nusselt number for a constant wall temperature, according to Eckert and Drake [4], is

$$Nu_x = f(m)Re_x^{1/2}Pr^{1/3}, \tag{A.3}$$

where $f(m) = 0.322$ for a plane wall ($m = 0$). The values of $f(m)$ from wedge flow analyses are plotted in Fig. 8. They were obtained from Figs. 7–10, p. 310, in Eckert and Drake [4]; they are also conveniently tabulated in Table 10-2 in Kays and Crawford [21].

$$\frac{Nu}{Sh} = f(m)\left(\frac{Pr}{Sc}\right)^{1/3}. \tag{A.4}$$

The function, $f(m)$, is nearly a constant for a specific flow process and Eq. (A.4) can be approximated by $F = Nu/Sh = (Pr/Sc)^{1/3}$ for a specified flow process. According to this equation, the local analogy factor is also equal to the average one, $F = \bar{F}$.

It has been established in Section 2 that there is no difference between local and average analogy factors, $Nu/Sh$, for laminar boundary layers. It will now be shown that this is also the case for turbulent ones.

Eq. (A.3) shows that $Nu_x$ is for wedge-type flow, with good approximation, a function of $m$ and, therefore, according to Eq. (A.1) a function of $x/C$. Eq. (A.3) can, therefore, be written as

$$Nu_x = Re_c^{1/2}Pr^{1/3}f_1(x/C). \tag{A.5}$$

In analogy, we write for a turbulent boundary layer

$$Nu_x = Re_c^m Pr^n f_2(x/C). \tag{A.6}$$

The average Nusselt number is

$$\overline{Nu} = \frac{C}{x_2 - x_1}Re_c^m Pr^n \int_{x_1/C}^{x_2/C} f_2(x/C). \tag{A.7}$$

Using the analogy operator in Eq. (4) of the introduction, Eqs. (A.6) and (A.7) express also the local and average Sherwood numbers when $Nu_x$ is replaced by $Sh_x$ and $\overline{Nu}$ by $\overline{Sh}$ and for the analogy factors, one obtains the equation

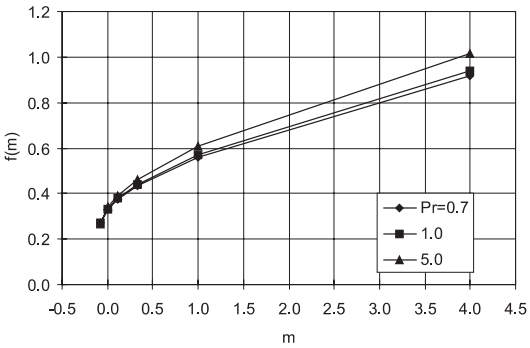


Fig. 8. Variations of $f(m)$ in Eq. (A.4) from the wedge flow solutions.

$$\frac{Nu_x}{Sh_x} = \frac{\overline{Nu}}{\overline{Sh}} \tag{A.8}$$

which is identical with Eq. (10).

## References


[1] E. Schmidt, Verdunstung und Wärmeübergang, Gesundheits-Ingenieur 29 (1929) 525–529.

[2] W. Nusselt, Wärmeübergang, Diffusion und Verdunstung, Math. Mechanik 2 (1930) 105–121.

[3] U. Grigull (Ed.), Selected Publications of Wilhelm Nusselt and Ernst Schmidt, Hemisphere, Washington, DC, 1982, pp. 109–125 and 164–168.

[4] E.R.G. Eckert, R.M. Drake Jr., Analysis of Heat and Mass Transfer, Hemisphere, Washington, DC, 1987, pp. 306–314 and 383.

[5] P.H. Chen, Measurement of local mass transfer from a gas turbine blade, Ph.D. thesis, University of Minnesota, Minneapolis, MN, 1988.

[6] P.H. Chen, R.J. Goldstein, Convective transport phenomena on the suction of a turbine blade including the influence of secondary flows near the endwall, J. Turbomachinery 114 (1992) 776–787.

[7] H.P. Wang, Local mass transfer measurement form a turbine blade: influence of high turbulence with large length scale on heat/mass transfer, Ph.D. thesis, University of Minnesota, Minneapolis, MN, 1997.

[8] M.E. Crawford, W.M. Kays, STAN5: A program for numerical computation of two-dimensional internal and external boundary layer flows, NASA Technical Reports, CR-2742, 1976.

[9] E.R.G. Eckert, Similarity analysis of model experiments for film cooling in gas turbines, Wärme und Stoffübertragung 27 (1992) 217–223.

[10] O. Reynolds, On the dynamical theory of incompressible viscous fluids and the determination of the criterion, Phil. Trans. Roy. Soc. A 186 (1895) 123–164.

[11] O. Reynolds, Scientific Papers, Cambridge University Press, Cambridge, 1895, p. 535.

[12] O. Reynolds, D. McDonald, J.D. Jackson (Eds.), Osborn Reynolds and Engineering Science Today, Manchester University Press, Manchester, 1970.

[13] R.J. Goldstein, H.H. Cho, A review of mass transfer measurements using naphthalene sublimation, Exp. Thermal and Fluid Sci. 10 (1995) 416–434.

[14] M. Häring, B. Weigand, A new analogy function for the naphthalene sublimation technique to measure heat transfer coefficients on turbine airfoils, ASME Paper# 95-GT-17, 1995.

[15] M. Häring, A. Hoffs, A. Bolcs, B. Weigand, An experimental study to compare the naphthalene sublimation with the liquid crystal technique in compressible flow, ASME Paper# 95-GT-16, 1995.

[16] A. Hoffs, A. Bolcs, S. Harasgama, Transient heat transfer experiments in a linear cascade via an insertion mechanism using the liquid crystal technique, J. Turbomachinery 119 (1997) 9–13.

[17] J.T. Chung, T.W. Simon, Effectiveness of the gas turbine endwall fences in secondary flow control at elevated freestream turbulence levels, ASME Paper# 93-GT-51, 1993.

[18] J.T. Chung, Flow and heat transfer experiments in the turbine airfoil/endwall region, Ph.D. thesis, University of Minnesota, Minneapolis, MN, 1992.

[19] C. Camci, K. Kim, S. Hippensteele, A new hue capturing technique for the quantitative interpretation of liquid crystal images used in convective heat transfer studies, ASME Paper# 91-GT-122, 1991.

[20] R.J. Goldstein, E.R.G. Eckert, H.P. Wang, S.J. Olson, Effects of Blade Profile on Turbine Blade Heat (Mass) Transfer, Process, Enhanced and Multiphase Heat Transfer – A Symposium in Honor of Professor Arthur E. Bergles, Georgia Institute of Technology, Atlanta, GA, 16 November 1996.

[21] W.M. Kays, M.E. Crawford, Convective Heat and Mass Transfer, McGraw-Hill, New York, 1996, p. 167.